Design and Characterization of Bioinstructive Gold Nanocomposite Hydrogels for 3D Bioprinting

Representative images of the lyophilized nanoparticle formulations are presented in Supplementary Figure S1A. The unmodified AuNPs exhibited visible aggregation following freeze-drying, whereas PEG- and PEG-GSH-functionalized nanoparticles showed improved dispersion and reconstitution behavior. To further evaluate post-lyophilization stability, the freeze-dried nanoparticles were rehydrated in Milli-Q water and GlutaMAX culture medium, followed by UV–Vis absorbance analysis (Supplementary Figure S1B).

The reconstituted AP and APG formulations retain characteristic absorbance features associated with AuNP surface plasmon resonance, indicating preservation of nanoparticle integrity after freeze-drying and rehydration. In contrast, the unmodified AuNP group demonstrated reduced optical stability and increased aggregation behavior following reconstitution. These findings further support the stabilizing role of PEG and GSH functionalization in maintaining nanoparticle dispersion and physicochemical stability under storage and rehydration conditions relevant to downstream biofabrication and biological applications.

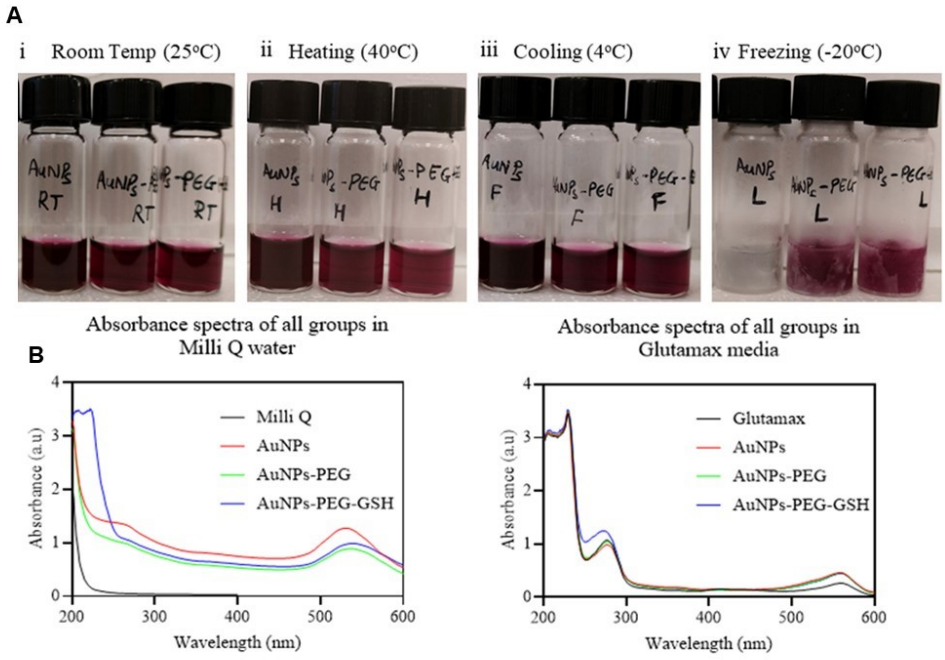

Figure S1: Lyophilization stability and reconstitution behavior of AuNP, AuNPs-PEG, and AuNPs-PEG-GSH formulations.

Cytocompatibility of AuNPs and GSH on PDLSCs

AuNPs have been demonstrated to improve stem cell proliferation by providing a supportive environment for cell adhesion, migration, and proliferation. Their nanoscale dimensions allow for enhanced cellular uptake and interactions, leading to increased cell viability and proliferation rates[44]. To assess the processing efficiency and overall cytocompatibility of the synthesized AuNPs and GSH on PDLSCs cell viability (an MTS) assay was conducted. PDLSCs were grown as monolayers and exposed to different concentrations of AuNPs and GSH. This assay was performed following the ISO 10993-5 standards (Biological evaluation of medical devices), which require at least 70% cell viability in comparison to the control. The results confirmed that the minimum safe concentration for enhancing cell viability beyond 70% was 10 µg/ml AuNPs (Figure 1SA and C), which was subsequently selected for use. Furthermore, considering the role of GSH as a potent antioxidant, its maximum concentration was determined based on the maintenance of cell viability and health. Through this assay, we observed that 20 mM facilitated cell proliferation while preserving cellular morphology (Figure 1SB and C).

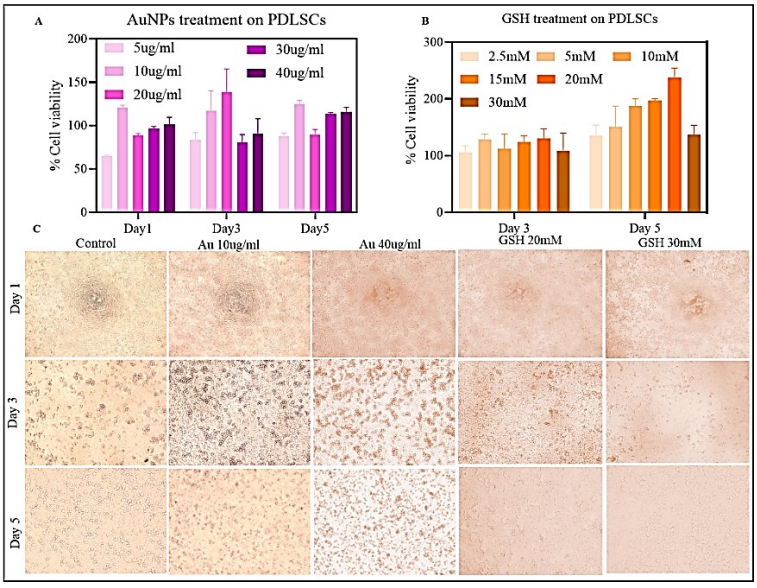

Figure S2: Cell Viability Assay for AuNPs and GSH Treatment on PDLSCs (A) AuNPs MTS assay (B) GSH MTS assay (C) Pictures of cell morphology at Day 1, 3 and 5 after treatment.

Temperature-Dependent Rheological Behaviour of GelMA-Based Bioinks

To further investigate the thermal rheological behavior of the developed bioinks, temperature sweep analyses were performed to evaluate changes in complex viscosity and viscoelastic moduli with increasing temperature (Supplementary Figure S2). All formulations exhibited a gradual reduction in complex viscosity as temperature increased, indicating temperature-dependent softening of the GelMA network (Supplementary Figure S2A). A more pronounced decrease in viscosity was observed near 20–23 °C,

consistent with reduced intermolecular interactions and increased polymer-chain mobility at elevated temperatures.

The viscoelastic response of the formulations was further evaluated by monitoring the storage modulus (G′) and loss modulus (G″) during temperature ramping (Supplementary Figure S2B). All groups demonstrated progressive decreases in both G′ and G″ with increasing temperature, reflecting weakening of the physically crosslinked hydrogel structure. Despite thermal softening, nanoparticle-containing formulations maintained comparable viscoelastic profiles relative to GelMA alone, supporting their suitability for temperature-responsive extrusion-based bioprinting applications.

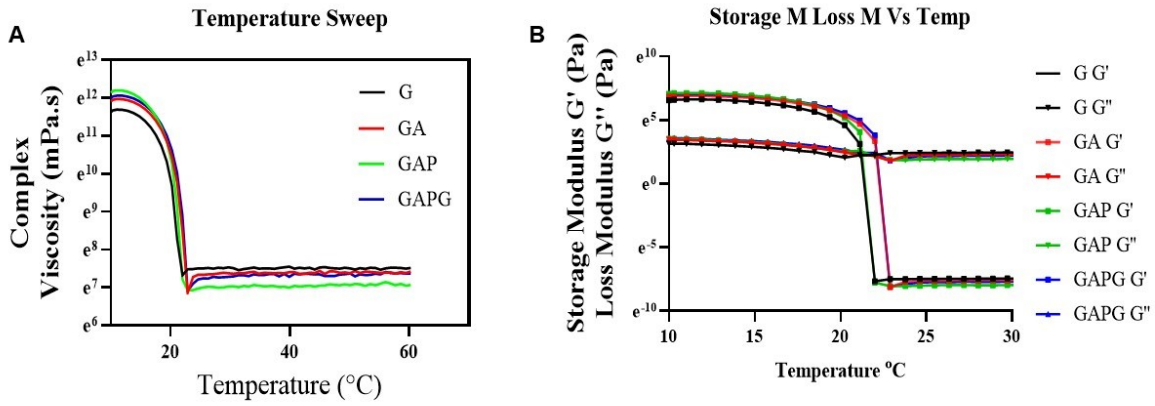

Figure S3: Temperature-dependent rheological characterization of GelMA-based bioinks. (A) Complex viscosity profiles of G, GA, GAP, and GAPG formulations during temperature sweep analysis. (B) Temperature-dependent storage modulus (G′) and loss modulus (G″) behavior of the bioink formulations.

Alizarin Red S Staining

Representative wide-field Alizarin Red S staining images of the bioprinted constructs are presented in Supplementary Figure S3. All formulations demonstrated evidence of mineralized matrix deposition under basal culture conditions at both Day 7 and Day 14. Qualitative variations in staining distribution and mineralized nodule formation were observed among the groups, particularly in nanoparticle-containing formulations.

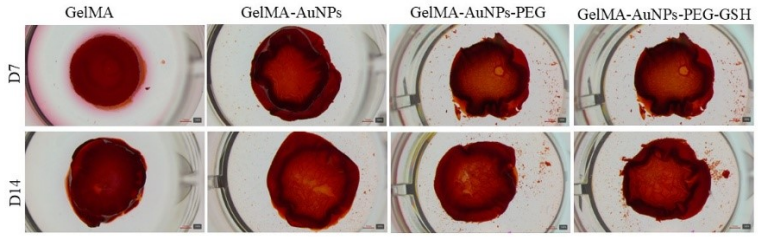

Fig 4: Representative Macroscopic image of Alizarin Red S staining of bioprinted constructs